arXiv:1009.1958v2 [gr-qc] 22 Jun 2011

Thin accretion disk signatures of slowly rotating black holes in Hořava gravity

Tiberiu Harko* and Zoltán Kovács†

Department of Physics and Center for Theoretical and Computational Physics, The University of Hong Kong, Pok Fu Lam Road, Hong Kong

Francisco S. N. Lobo‡

Centro de Astronomia e Astrofísica da Universidade de Lisboa, Campo Grande, Ed. C8 1749-016 Lisboa, Portugal

(Dated: June 23, 2011)

In the present work, we consider the possibility of observationally testing Hořava gravity by using the accretion disk properties around slowly rotating black holes of the Kehagias-Sfetsos solution in asymptotically flat spacetimes. The energy flux, temperature distribution, the emission spectrum as well as the energy conversion efficiency are obtained, and compared to the standard slowly rotating general relativistic Kerr solution. Comparing the mass accretion in a slowly rotating Kehagias-Sfetsos geometry in Hořava gravity with the one of a slowly rotating Kerr black hole, we verify that the intensity of the flux emerging from the disk surface is greater for the slowly rotating Kehagias-Sfetsos solution than for rotating black holes with the same geometrical mass and accretion rate. We also present the conversion efficiency of the accreting mass into radiation, and show that the rotating Kehagias-Sfetsos solution provides a much more efficient engine for the transformation of the accreting mass into radiation than the Kerr black holes. Thus, distinct signatures appear in the electromagnetic spectrum, leading to the possibility of directly testing Hořava gravity models by using astrophysical observations of the emission spectra from accretion disks.

PACS numbers: 04.50.Kd, 04.70.Bw, 97.10.Gz

I. INTRODUCTION

Recently, Hořava proposed a renormalizable gravity theory in four dimensions which reduces to Einstein gravity with a non-vanishing cosmological constant in IR but with improved UV behaviors [1, 2]. The latter theory admits a Lifshitz scale-invariance in time and space, exhibiting a broken Lorentz symmetry at short scales, while at large distances higher derivative terms do not contribute, and the theory reduces to standard general relativity (GR). Since then various properties and characteristics of the Hořava gravities have been extensively analyzed, ranging from formal developments [3], cosmology [4], dark energy [5] and dark matter [6], and spherically symmetric solutions [7, 10–12]. Although a generic vacuum of the theory is anti-de Sitter one, particular limits of the theory allow for the Minkowski vacuum. In this limit the leading order the Parameterized post-Newtonian (PPN) coefficients coincide with those of the pure GR. Thus, the deviations from the conventional GR can be tested only beyond the post-Newtonian corrections, that is for a system with strong gravity at astrophysical scales.

There are basically four versions of Hořava gravity, namely, those with or without the "detailed balance condition", and with or without the "projectability condition". The "detailed balance condition" restricts the form of the potential in the 4–dim Lorentzian action to a specific form in terms of a 3–dim Euclidean theory. In a cosmological context, this condition leads to obstacles, and thus must be abandoned. In this context, the 'soft' violation of the 'detailed balance' condition modifies the IR behavior. This IR modification, with an arbitrary cosmological constant, represent the analogs of the standard Schwarzschild-(A)dS solutions, which were absent in the original Hořava model. The "projectability condition" essentially stems from the fundamental symmetry of the theory, i.e., the foliation-preserving diffeomorphism invariance, and must be respected. Foliation-preserving diffeomorphism consists of a 3–dim spatial and the space-independent time reparametrization.

IR-modified Hořava gravity seems to be consistent with the current observational data [14–16], but in order to test its viability more observational constraints are necessary. In [17] the possibility of observationally testing Hořava gravity was considered by using the accretion disk properties around black holes. The energy flux, temperature distribution, the emission spectrum as well as the energy conversion efficiency are obtained, and compared to the standard general relativistic case. It was shown that particular signatures can appear in the electromagnetic spectrum, thus leading to the possibility of directly testing Hořava gravity models by using astrophysical observations of the emission spectra from accretion disks. In this paper, we further explore the possibility of testing the viability of Hořava-Lifshitz gravity using thin accretion disk properties, and we generalize the previous results from [17] to the case of the slowly rotating Hořava-Lifshitz black holes. As for the slowly rotating Hořava-Lifshitz black hole, we adopt the solution obtained in

*Electronic address: harko@hkucc.hku.hk
†Electronic address: zkovacs@hku.hk
‡Electronic address: flobo@cii.fc.ul.pt

[18], and we carry out an analysis of the properties of the radiation emerging from the surface of the disk. For more information on thin accretion disks around compact objects we refer the reader to Refs. [19–35].

It seems to be an extremely difficult endeavor to find a fully rotating black hole in Hořava-Lifshitz theory as the full equations to be solved are very complicated, so only the slowly rotating regime is analyzed in this work. Note that the "slowly rotating" black hole means that one considers up to linear order of the rotating parameter $a = J/M$ ($a \ll 1$) in the metric functions, equations of motion, and thermodynamic quantities [18]. It is also important to emphasize that the slowly rotating Kerr black hole is recovered from the slowly rotating black hole solutions in Hořava gravity, in the IR limit of $\omega \to \infty$. As compared to the standard general relativistic case, significant differences appear in the energy flux and electromagnetic spectrum for Hořava black holes, thus leading to the possibility of directly testing the Hořava-Lifshitz theory by using astrophysical observations of the emission spectra from accretion disks.

The present paper is organized as follows. In Sec. II, we present the action and the specific solution of slowly rotating black holes. In Sec. III, we present some essential thermal equilibrium radiation properties of thin accretion disks in stationary axisymmetric spacetimes. In Sec. IV, we analyze the basic properties of matter forming a thin accretion disk around vacuum black holes in Hořava gravity, and compare the results with the slowly rotating Kerr solution. We discuss and conclude our results in Sec. V. Furthermore, for self-completeness and self-consistency, we review the formalism and the physical properties of the thin disk accretion onto compact objects in Appendix A.

II. SLOWLY ROTATING BLACK HOLES IN HOŘAVA GRAVITY

In this section, we briefly review the Hořava-Lifshitz theory, where differential geometry of foliations represents the proper mathematical setting for the class of gravity theories studied by Hořava [2]. Thus, it is useful to use the ADM formalism, where the four-dimensional metric is parameterized by the following

$$ds^2 = -N^2 c^2\, dt^2 + g_{ij}\left(dx^i + N^i\, dt\right)\left(dx^j + N^j\, dt\right)\,, \quad (1)$$

where N is the lapse function, N^i, the shift vector, and g_{ij} the 3-dimensional spatial metric.

In this context, the Einstein-Hilbert action is given by

$$S = \frac{1}{16\pi G}\int d^4x\, \sqrt{g}\, N\left(K_{ij}K^{ij} - K^2 + R^{(3)} - 2\Lambda\right), \quad (2)$$

where G is Newton's constant, $R^{(3)}$ is the three-dimensional curvature scalar for g_{ij}. The extrinsic curvature, K_{ij}, is defined as

$$K_{ij} = \frac{1}{2N}\left(\dot{g}_{ij} - \nabla_i N_j - \nabla_j N_i\right), \quad (3)$$

where the dot denotes a derivative with respect to t, and ∇_i is the covariant derivative with respect to the spatial metric g_{ij}.

The IR-modified Hořava action is given by

$$\begin{aligned} S \;=\; & \int dt\, d^3x\, \sqrt{g}\, N\Bigg[\frac{2}{\kappa^2}\left(K_{ij}K^{ij} - \lambda K^2\right) - \frac{\kappa^2}{2\nu^4}C_{ij}C^{ij} \\ & + \frac{\kappa^2\mu}{2\nu^2}\epsilon^{ijk}R^{(3)}_{il}\nabla_j R^{(3)l}{}_k - \frac{\kappa^2\mu^2}{8}R^{(3)}_{ij}R^{(3)ij} \\ & + \frac{\kappa^2\mu^2}{8(3\lambda-1)}\left(\frac{4\lambda-1}{4}(R^{(3)})^2 - \Lambda_W R^{(3)} + 3\Lambda_W^2\right) \\ & + \frac{\kappa^2\mu^2\omega}{8(3\lambda-1)}R^{(3)}\Bigg], \end{aligned} \quad (4)$$

where κ, λ, ν, μ, ω and Λ_W are constant parameters. C^{ij} is the Cotton tensor, defined as

$$C^{ij} = \epsilon^{ikl}\nabla_k\left(R^{(3)j}{}_l - \frac{1}{4}R^{(3)}\delta^j_l\right). \quad (5)$$

The last term in Eq. (4) represents a 'soft' violation of the 'detailed balance' condition, which modifies the IR behavior. This IR modification term, $\mu^2 R^{(3)}$, generalizes the original Hořava model (we have used the notation of Ref. [10]).

The fundamental constants of the speed of light c, Newton's constant G, and the cosmological constant Λ are defined as

$$c^2 = \frac{\kappa^2\mu^2|\lambda_W|}{8(3\lambda-1)^2} \quad G = \frac{\kappa^2 c^2}{16\pi(3\lambda-1)} \quad \Lambda = \frac{3}{2}\Lambda_W c^2. \quad (6)$$

Consider the static and spherically symmetric metric given by

$$ds^2 = -N^2(r)\, dt^2 + \frac{dr^2}{f(r)} + r^2\left(d\theta^2 + \sin^2\theta\, d\phi^2\right), \quad (7)$$

where $N(r)$ and $f(r)$ are arbitrary functions of the radial coordinate, r.

Imposing the specific case of $\lambda = 1$, $\beta = 4\omega M$ (M is the mass parameter) and $\Lambda_W = 0$, one obtains the Kehagias and Sfetsos's (KS) asymptotically flat solution [12], given by

$$f_{\rm KS} = N^2_{\rm KS} = 1 + \omega r^2\left(1 - \sqrt{1 + \frac{4M}{\omega r^3}}\right). \quad (8)$$

In the limit of $\omega \to \infty$, it reduces to the Schwarzschild form.

Note that there is an outer (event) horizon, and an inner (Cauchy) horizon at

$$r_\pm = M\left[1 \pm \sqrt{1 - 1/(2\omega M^2)}\right]. \quad (9)$$

To avoid a naked singularity at the origin, one also needs to impose the condition

$$\omega M^2 \geq \frac{1}{2}. \quad (10)$$

Note that in the GR regime, i.e., $\omega M^2 \gg 1$, the outer horizon approaches the Schwarzschild horizon, $r_+ \simeq 2M$, and the inner horizon approaches the central singularity, $r_- \simeq 0$.

In the present work we propose to study the thin accretion disk models applied for slowly rotating black holes in Hořava-Lifshitz gravity models [18], and carry out an analysis of the properties of the radiation emerging from the surface of the disk. It does indeed seem to be a formidable task to find a fully rotating black hole in Hořava-Lifshitz theory as the full equations to be solved are very complicated, so only the slowly rotating regime is analyzed in this work. Note that the "slowly rotating" black hole means that one considers up to linear order of the rotating parameter $a = J/M$ ($a \ll 1$) in the metric functions, equations of motion, and thermodynamic quantities. In this work we use the results obtained in Ref. [18], where the slowly rotating black hole is interpreted as arising from the breaking of spherical to axial symmetry. Rather than reproduce the analysis carried out, we refer to reader to Ref. [18] for details.

Thus, the slowly rotating black hole solution obtained in [18] is given by

$$\begin{aligned} ds^2_{\text{slow KS}} &= -f_{\text{KS}}(r)dt^2 + \frac{dr^2}{f_{\text{KS}}(r)} + r^2 d\theta^2 \\ &\quad + r^2 \sin^2\theta \left(d\phi^2 - \frac{4J}{r^3} dt d\phi \right) , \end{aligned} \tag{11}$$

where the factor $f_{\text{KS}}(r)$ reduces to the KS solution, and is given by Eq. (8).

For self-completeness and self-consistency, the Kerr black hole is also presented

$$ds^2_{\text{Kerr}} = -\frac{\rho^2 \Delta_r}{\Sigma^2} dt^2 + \frac{\rho^2}{\Delta_r} dr^2 + \rho^2 d\theta^2 + \frac{\Sigma^2 \sin^2\theta}{\rho^2} \left(d\phi - \xi dt \right)^2 , \tag{12}$$

where

$$\begin{aligned} \rho^2 &= r^2 + a^2 \cos^2\theta, \\ \Delta_r &= \left(r^2 + a^2\right) - 2Mr, \\ \Sigma^2 &= \left(r^2 + a^2\right)^2 - a^2 \sin^2\theta \Delta_r, \\ \xi &= \frac{2Mar}{\Sigma^2}. \end{aligned} \tag{13}$$

In the slowly rotating limit of $J \ll M (a \ll 1)$, the Kerr solution reduces to

$$\begin{aligned} ds^2_{\text{slow Kerr}} &= -\Big(1 - \frac{2M}{r}\Big) dt^2 + \frac{dr^2}{\left(1 - \frac{2M}{r}\right)} + r^2 d\theta^2 \\ &\quad + r^2 \sin^2\theta \Big(d\phi^2 - \frac{4J}{r^3} dt d\phi \Big) \end{aligned} \tag{14}$$

It was argued in [18] that the slowly rotating Kerr black hole could be interpreted as arising from the breaking of spherical to axial symmetry. It is easily checked that in the limit of $\omega \to \infty$, the slowly rotating solution (11) leads to the slowly rotating Kerr solution (14). In the analysis of the thin disk properties that follow, we compare the geometries given by the metrics (11) and (14), respectively.

III. GEODESIC MOTION OF TEST PARTICLES IN SLOWLY ROTATING KEHAGIAS-SFETSOS GEOMETRY

In this section we consider the thermal radiation properties of thin accretion disks in stationary axisymmetric spacetimes. The formalism has been extensively presented in the literature. However, in order to analyze the electromagnetic signatures of thin accretion disks around slowly rotating black holes, for self-completeness and self-consistency, we consider the main results of stationary and axially symmetric spacetimes in this section and the physical properties of accretion disks in Appendix A.

The physical properties and the electromagnetic radiation characteristics of particles moving in circular orbits around compact bodies are determined by the geometry of the spacetime around the compact object. For a stationary and axially symmetric geometry the metric is given in a general form by

$$ds^2 = g_{tt}\, dt^2 + 2g_{t\phi}\, dt d\phi + g_{rr}\, dr^2 + g_{\theta\theta}\, d\theta^2 + g_{\phi\phi}\, d\phi^2 \, . \tag{15}$$

In the equatorial approximation, i.e., $|\theta - \pi/2| \ll 1$, which is the case of interest for our analysis, the metric functions g_{tt}, $g_{t\phi}$, g_{rr}, $g_{\theta\theta}$ and $g_{\phi\phi}$ only depend on the radial coordinate r.

To compute the relevant physical quantities of the thin accretion disks, we determine first the radial dependence of the angular velocity Ω, of the specific energy $\widetilde{E}$, and of the specific angular momentum $\widetilde{L}$, respectively, of particles moving in circular orbits in a stationary and axially symmetric geometry. The geodesic equations of the motion take the following form

$$\frac{dt}{d\tau} = \frac{\widetilde{E} g_{\phi\phi} + \widetilde{L} g_{t\phi}}{g_{t\phi}^2 - g_{tt} g_{\phi\phi}}, \tag{16}$$

$$\frac{d\phi}{d\tau} = -\frac{\widetilde{E} g_{t\phi} + \widetilde{L} g_{tt}}{g_{t\phi}^2 - g_{tt} g_{\phi\phi}}, \tag{17}$$

$$g_{rr} \left(\frac{dr}{d\tau} \right)^2 = -1 + \frac{\widetilde{E}^2 g_{\phi\phi} + 2\widetilde{E}\widetilde{L} g_{t\phi} + \widetilde{L}^2 g_{tt}}{g_{t\phi}^2 - g_{tt} g_{\phi\phi}}. \tag{18}$$

From Eq. (18) one can introduce an effective potential term as

$$V_{eff}(r) = -1 + \frac{\widetilde{E}^2 g_{\phi\phi} + 2\widetilde{E}\widetilde{L} g_{t\phi} + \widetilde{L}^2 g_{tt}}{g_{t\phi}^2 - g_{tt} g_{\phi\phi}}. \tag{19}$$

For stable circular orbits in the equatorial plane the following conditions must hold: $V_{eff}(r) = 0$ and $V_{eff,\,r}(r) = 0$, where the comma in the subscript denotes a derivative with respect to the radial coordinate r.

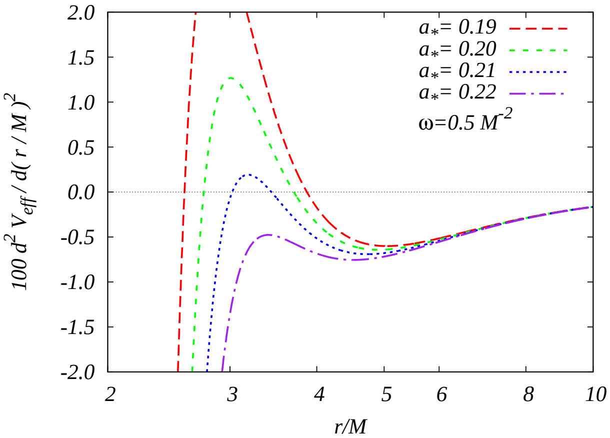

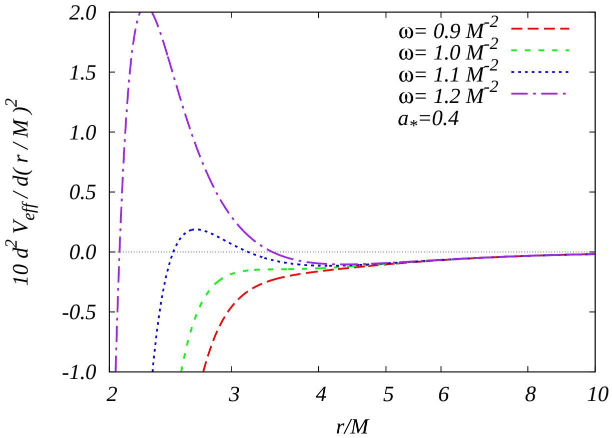

FIG. 1: The second order derivative of the effective potential with respect to (r/M) for a slowly rotating KS black hole with total mass M for different values of the parameters ω and a_*.

These conditions provide the specific energy, the specific angular momentum and the angular velocity of particles moving in circular orbits for the case of spinning general relativistic compact spheres, given by

$$\widetilde{E} = -\frac{g_{tt}+g_{t\phi}\Omega}{\sqrt{-g_{tt}-2g_{t\phi}\Omega-g_{\phi\phi}\Omega^2}}, \quad (20)$$

$$\widetilde{L} = \frac{g_{t\phi}+g_{\phi\phi}\Omega}{\sqrt{-g_{tt}-2g_{t\phi}\Omega-g_{\phi\phi}\Omega^2}}, \quad (21)$$

$$\Omega = \frac{d\phi}{dt} = \frac{-g_{t\phi,r}+\sqrt{(g_{t\phi,r})^2-g_{tt,r}g_{\phi\phi,r}}}{g_{\phi\phi,r}}. \quad (22)$$

The marginally stable orbit around the central object can be determined from the condition $V_{eff,\,rr}(r)=0$. To this effect, we formally represent the effective potential as

$$V_{eff}(r) \equiv -1+\frac{f}{g},$$

where

$$f \equiv \widetilde{E}^2 g_{\phi\phi} + 2\widetilde{E}\widetilde{L}g_{t\phi} + \widetilde{L}^2 g_{\phi\phi},$$
$$g \equiv g_{t\phi}^2 - g_{tt}g_{\phi\phi},$$

and where the condition $g \neq 0$ is imposed. From $V_{eff}(r)=0$, we obtain first $f=g$. The condition $V_{eff,\,r}(r)=0$ provides $f_{,r}g-fg_{,r}=0$. Thus, from these conditions one readily derives $V_{eff,\,rr}(r)=0$, which provides the following important relationship

$$\begin{aligned} 0 &= (g_{t\phi}^2-g_{tt}g_{\phi\phi})V_{eff,rr} \\ &= \widetilde{E}^2 g_{\phi\phi,rr} + 2\widetilde{E}\widetilde{L}g_{t\phi,rr} + \widetilde{L}^2 g_{tt,rr} \\ &\quad -(g_{t\phi}^2-g_{tt}g_{\phi\phi})_{,rr}\ , \end{aligned} \quad (23)$$

where $g_{t\phi}^2-g_{tt}g_{\phi\phi}$ (appearing as a cofactor in the metric determinant) never vanishes. By inserting Eqs. (20)-(22) into Eq. (23) and solving this equation for r, we obtain the radii of the marginally stable orbits, once the metric coefficients g_{tt}, $g_{t\phi}$ and $g_{\phi\phi}$ are explicitly given.

In the context of the slowly rotating KS black hole given by the metric (11), and considering the equatorial approximation ($|\theta-\pi/2|\ll 1$) of the geometry, the particles moving in Keplerian orbits around the slowly rotating black hole have the following specific energy, specific angular momentum and angular velocity

$$\widetilde{E} = \frac{1+\omega r^2+2M^2a_*r^{-1}-\omega h r^2}{\sqrt{1+(\omega-\Omega^2)r^2+4Ma_*\Omega r^{-1}-\omega h r^2}}\ , \quad (24)$$

$$\widetilde{L} = \frac{r^2\Omega-2M^2a_*r^{-1}}{\sqrt{1+(\omega-\Omega^2)r^2+4Ma_*\Omega r^{-1}-\omega h r^2}}\ , \quad (25)$$

$$\Omega = \frac{\sqrt{h(M^4a_*^2+\omega r^6)-Mr^3-\omega r^6}-2M^2a_*\sqrt{h}}{2r^3\sqrt{h}} \quad (26)$$

respectively, where $a_*=J/M^2$ and $h=\sqrt{1+4M/(\omega r^3)}$ are defined for notational simplicity. By inserting these equations into the second order derivative (23) of the effective potential, we can determine the radii of the marginally stable orbits for different values of the spin parameter a_* and of the parameter ω. In order to obtain consistency with the metric, Eqs. (24)-(26) should be linearized with respect to the parameter $a_*=J/M^2$. However, since $\widetilde{E}$, $\widetilde{L}$ and Ω are constants of motion, their numerical values are also obtained from the particular values given to a_* and ω, respectively. Therefore any series expansion or linearization of Eqs. (24)-(26) will just slightly modify the numerical values of the constants of motion, without significantly affecting the physical results.

In Fig. 1 we plot the quantity $d^2V_{eff}/d(r/M)^2$ as a function of the dimensionless radius r/M. The left plot shows the radial profile of the second order derivative calculated for different values of a_* in a narrow range between 0.19 and 0.22 at a fixed value of ω (set to its the minimal value $1/2M^2$). For $a_*=0.19$, 0.20 and 0.21, $d^2V_{eff}/d(r/M)^2$ has zeroes, and the larger value

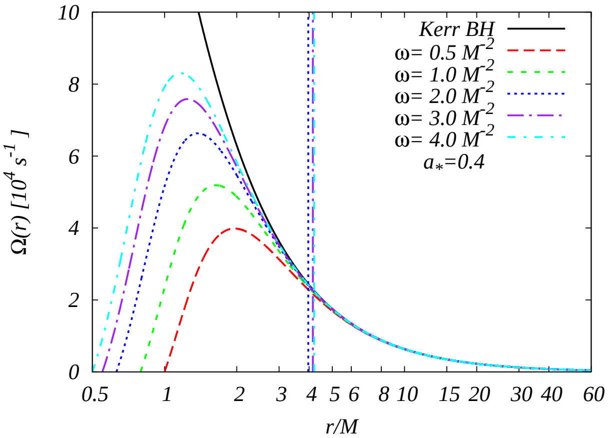

FIG. 2: The rotational velocity of the Keplerian orbits in the equatorial plane as a function of (r/M) for a slowly rotating KS black hole with total mass $1M_\odot$ for different values of the parameters ω and $a_* = 0.4$. The vertical lines indicate the location of the ISCO for those discs for which it exists.

of the root provides the radius r_{ms} of the marginally stable orbit. But the second derivative of the effective potential, calculated for $a_* = 0.22$, remains negative for any $r > r_+$. Hence stable circular orbits do exist for $a_* = 0.22$ and $\omega = 1/2M^2$ in the entire equatorial plane outside the horizon ($r_\pm = M$). The critical value of a_* above which no marginally stable orbit exists depends on ω. The right hand side plot in Fig. 1 shows that a given value of a_* becomes critical if we decrease ω: for $a_* = 0.4$, the second order derivative of V_{eff}, calculated at $\omega = 1.1M^{-2}$ and $1.2M^{-2}$, still has some roots, but there are no marginally stable orbits for $\omega = 1M^{-2}$ and $\omega = 0.9M^{-2}$, respectively. The presence of the critical value for a_*, and its numerical value, certainly depends on the approximation used to obtain the metric. Such a critical value may indicate a breakdown of the metric for enough high rotational velocities. For an exact solution and for high spins, the location of the stable circular orbits may be different. However, since the solution we are considering is valid for small a_* only, the extrapolation of our results to higher spin values may lead to unphysical results.

Another interesting property of the Keplerian motion around a slowly rotating KS black hole is the radial dependence of the orbital frequency of the particles, shown in Fig. 2. In Fig. 2 we plot Ω versus r/M for a fixed value of $a_* = 0.4$, and for different values of ω. With decreasing values of ω, the radial profiles of the angular velocity decrease at lower radii, as compared to the general relativistic case. As we approach the horizon, this decrease is not only a relative decrease, but the curves fall to zero, instead of following the increase of the general relativistic case. Hence Ω has a maximal value for each pair of the parameters a_* and ω, as opposed to the angular velocity of the particles rotating around a Kerr black hole, where Ω remains a monotonous increasing function as we approach the horizon.

IV. ELECTROMAGNETIC SIGNATURES OF ACCRETION DISKS AROUND SLOWLY ROTATING KS BLACK HOLES

In this section we analyze the electromagnetic signatures of accretion disks around the slowly rotating KS black hole. We rely heavily on the formalism of the physical properties of thin accretion disks outlined in Appendix A.

In Fig. 3 we present the time-averaged fluxes of radiant energy $F(r)$ released from the accretion disks rotating around slowly rotating KS black holes. The fluxes were calculated by using Eqs. (24)-(26) in the flux integral Eq. (A7). The fluxes depend on two basic parameters, namely, the dimensionless spin parameter of the black hole, defined by $a_* = J/M^2$, and the free parameter ω, which appears in the solution given by Eq. (8). For a fixed total mass, $M = 1M_\odot$, and accretion rate, $\dot{M}_0 = 10^{-12}M_\odot/\mathrm{yr}$, in Fig. 3 we present the radial distributions of F for different values of a_* and ω. For comparison, we also plot the flux profiles for accretion disks around general relativistic black holes with the corresponding mass and spin parameter. The first plot shows the static case, which was already discussed in [17]. With the decreasing value of the parameter ω, the deviation of the spacetime geometry of the KS black hole from the geometry of the Schwarzschild black hole is enhanced. As a result, the flux profiles exhibit higher and higher differences. For low values of ω we obtain a higher maximal flux, as the inner edge of the accretion disk is shifted to lower radii (left edges of the flux profiles in the plots). The location of the flux maximum has a similar shift: with decreasing ω, F_{max} is shifted to lower radii. By comparing the flux maxima we see that F_{max} is about 1.4 times higher for the minimal value of ω than the maximum derived for the Schwarzschild black hole ($\omega \to \infty$).

Similar trends can be found for the slowly rotating cases shown in the rest of the plots of Fig. 3. For $a_* = 0.2$, the configurations with decreasing values of ω produce higher and higher flux values. The increase in the fluxes are again due to the increase in the surface of the accretion disk around the rotating KS black holes. These increase is clearly indicated by the large shifts of the inner disk edge to lower radii. Comparing these figures with the static case, both the shift of the inner edge and the enhancement in the flux amplitudes are much higher for the same values of ω: for $\omega = 0.5M^{-2}$, the maximal flux is already more than two times higher than F_{max} derived for the slowly rotating Kerr solution. By further increasing a_*, we can also increase the effect of the variation of ω on the radial structure of the standard thin accretion disk. We have seen that there is a critical value of the spin parameter for each ω, above which no marginally stable orbits can exist outside the horizon of

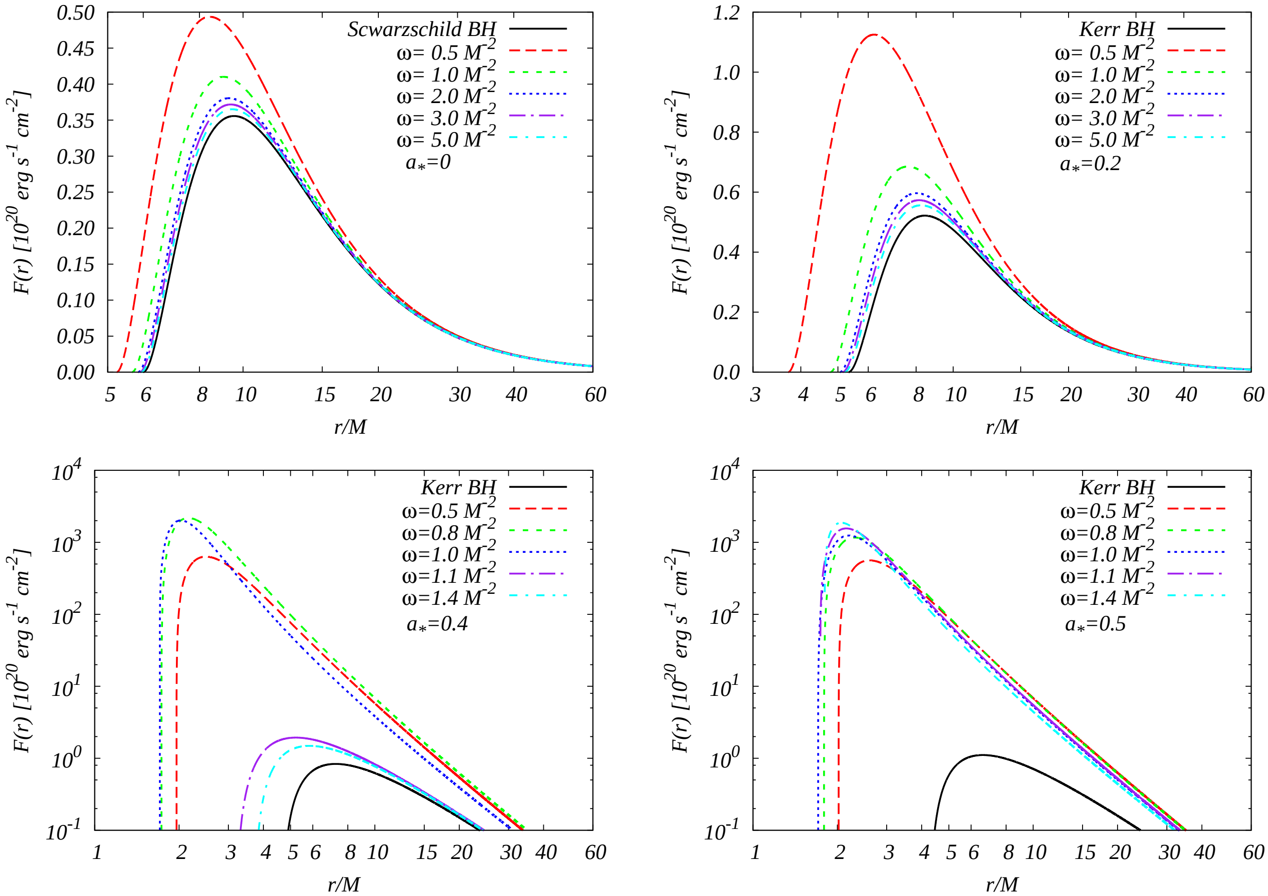

FIG. 3: The energy flux $F(r)$ radiated by the disk around a static and a slowly rotating KS black hole with the total mass of $1M_{\odot}$ for different values of the parameters ω and a_{*}. The mass accretion rate is set to $10^{-12}M_{\odot}$/yr.

the Kehagias-Safest black holes. If a_* exceeds this critical value, then the inner edge of the accretion disk is already located at the horizon, and the disk surface is considerably increased, as compared to the configuration with the spin parameter somewhat lower than the critical value. As a result, the amplitudes of the integrated flux have an enormous increase, i.e, there is a strong enhancement in the thermal radiation released from the disk surface.

A deeper physical interpretation of the breakdown of the standard accretion disk model for $< r_{max}$ may be associated with these high flux values. Some composite accretion disk models consider a geometrically thick and optically thin hot corona, positioned between the marginally stable orbit and the inner edge of the geometrically thin, and optically thick, accretion disk, where an inner edge is lying at a few gravitational radii [38]. In other type of composite models, the corona lies above and under the accretion disk, and the soft photons, arriving from the disk, produce a hard emission via their inverse comptonization by the thermally hot electrons in the corona [39]. In both configurations, the disk is truncated at several gravitational radii - reducing the soft photon flux of the disk - and the soft and hard components of the broad band X-ray spectra of black holes were attributed to the thermal radiation of the accretion disk and the emission mechanism in the corona, respectively. For KS black holes the innermost region of the disk with $r < r_{max}$ may indicate the presence of a hot corona where the rest mass accretion together with the energy and the angular momentum transport from the disk for $r > r_{max}$ to the region of the corona at lower radii cannot be described with the geometrically thin disk scheme. Thermal cooling of the corona via radiation is not able to maintain a thermodynamical equilibrium and the transport processes are dominated by heat conduction in the outer region of the corona or advection in a geometrically thick disk between r_+ and r_{max} in the core of the corona. In order to give a detailed description of the mechanism driving matter, energy and angular momentum into the black hole in the innermost region, one should construct at least a semi-analytic model without vertical averaging of the physical quantities of the accretion disk.

Here we carry out the analysis of the presence of the critical behavior only in the framework of the standards Novikov-Thorne disk models, which can still provide useful information about the whole phenomenon. This effect can be seen in the last two plots in Fig. 3. Since for $\omega > 1.1M^{-2}$ the value $a_* = 0.4$ is still under the critical value of the spin parameter, the maximal flux has still a moderate increase. If we set ω to $1.0M^{-2}$ or higher values, $a_* = 0.4$ exceeds the critical spin value shown in Fig. 1, and the left edge of the flux profile is located at radii $\leq 2r/M$. Nevertheless, these radii are still much higher than r_+ obtained for the corresponding values of ω. This is due to the fact that the radius r_{max} at which Ω attains its maximal value is greater than r_+. For lower radii Ω is already decreasing, as shown in Fig. 2, and from Eq. (A7) we obtain negative flux values. As a possible physical interpretation we can state that although the inner disk edge can reach the horizon, in the region between r_+ and r_{max} no physical mechanism is available for the radiative cooling of the disk, and thermal photons cannot leave the disk surface. Close to the inner edge of the disk, other processes might play a role in cooling the disk, and the standard thin disk model likely breaks down in this region. For $r > r_{max}$ the latter model still seems to be a satisfying description, and thus we can assume that the disk is in the state of the thermal equilibrium or at least very close to it.

If for a given ω the spin exceeds the critical value, then the minimal radius of the radiating disk surface is determined by the location of the Keplerian orbit with the maximal rotational frequency. As Fig. 2 shows, the value of the radial coordinate at which Ω is maximal is proportional to ω. Hence, this radius is maximal for the minimal value of ω, and the disk surface emitting thermal photons is minimal. Then, above the critical spin value, the relation between the flux maxima and the value of the parameter ω is inverted in comparison with the trends found below the critical spin value. This means that the higher the value of ω (the smaller the deviation from the general relativistic geometry), the higher the value of the maximal flux, and the lower the radial coordinate of the inner edge of the radiating zone.

At the limit $a_* = 0.5$ of the slow rotating regime, the flux maximum is three orders of magnitudes higher for $\omega = 1.4M^{-2}$ than the maximal value of $F(r)$ obtained for Kerr black holes. For all the values of ω presented in the last plot the spin value is higher than the critical value and each configuration of the thin disk rotating around the KS black hole emits much more thermal photons than the disk rotating around the Kerr black hole do. This holds even for the minimal value of ω. For $\omega \gg 1$ we can still reach the limit above which a_* is no longer greater than the critical spin value, and we can approach the lower flux values, which are typical for general relativistic black holes.

This enhancement in the sensitivity of the variation of ω can be studied in the radial profiles of the disk temperature as well. In Fig. 4 we present the distribution of the disk temperature for the same values of the parameters a_* and ω used in Fig. 3. As compared to the static case, in the case of the configuration with $a_* = 0.5$, we see a considerable increase in the disk temperature as a function of ω.

For the same set of the parameters a_* and ω we also plot the disk spectra in Fig. 5, which were calculated by applying Eq. (A9). The trends found in the behavior of the radial distribution of the radiant energy flux and disk temperature can also be seen here. For static spacetimes the disk spectra do not exhibit a strong sensitivity with the variation of ω, and the spectral amplitudes and the cut-off frequency of the spectra have only a moderate increase with decreasing ω. However, for the slowly rotating cases up to $a_* = 0.5$, the cut-off frequency can be enhanced by decreasing the value of ω, and the maximal amplitudes have a moderate increase as compared with the general relativistic black holes.

In the cases where for a given ω, a_* exceeds the value of the critical spin, the differences are considerable, indicating that the accretion disks rotating around a slowly rotating KS black hole have bluer spectra than the disks rotating around a Kerr black hole with identical mass and spin parameter. Both the increase in the amplitude and the shift in the cut-off frequency is proportional to the radiating surface of the disk. Therefore, they are increased with decreasing ω, provided that the spin is smaller than the critical value corresponding to the given ω. This trend can be seen in the third plot in Fig. 5, for $a_* = 0.4$, when $\omega > M^{-2}$ holds. If the spin exceeds the critical value for a given ω, this trend is inverted, as already found in the case of the flux profiles, and the configuration with the minimal value of ω produces the smallest amplitudes and cut-off frequency of the spectrum. This behavior is shown by the curves obtained for $\omega < M^{-2}$ in the third plot in Fig. 5, and for each curve obtained for the slowly rotating KS black hole in the last plot in Fig. 5.

The flux and the emission spectrum of the accretion disks around compact objects satisfy some scaling relations, with respect to the simple scaling transformation of the radial coordinate, given by $r \to \widetilde{r} = r/M$, where M is the mass of the compact sphere. Generally, the metric tensor coefficients are invariant with respect to this transformation, while the specific energy, the angular momentum and the angular velocity transform as

$$\widetilde{E} \to \widetilde{E}, \qquad \widetilde{L} \to M\widetilde{L}, \tag{27}$$

and

$$\Omega \to \widetilde{\Omega}/M, \tag{28}$$

respectively. The flux scales as $F(r) \to F(\widetilde{r})/M^4$, giving the simple transformation law of the temperature as $T(r) \to T(\widetilde{r})/M$. By also rescaling the frequency of the emitted radiation as $\nu \to \widetilde{\nu} = \nu/M$, the luminosity of the disk is given by $L(\nu) \to L(\widetilde{\nu})/M$.

Following [23] we can introduce the scale invariant dimensionless coordinate $x = \sqrt{r/M}$. Then the function $h(r) = \sqrt{1 + 4M/(\omega r^3)}$ in Eqs. (24)-(26) can be written as $h(x) = \sqrt{1 + 4/(\tilde{\omega} x^6)}$ where $\tilde{\omega} = \omega M^2$ is a dimensionless parameter. As a consequence, only the

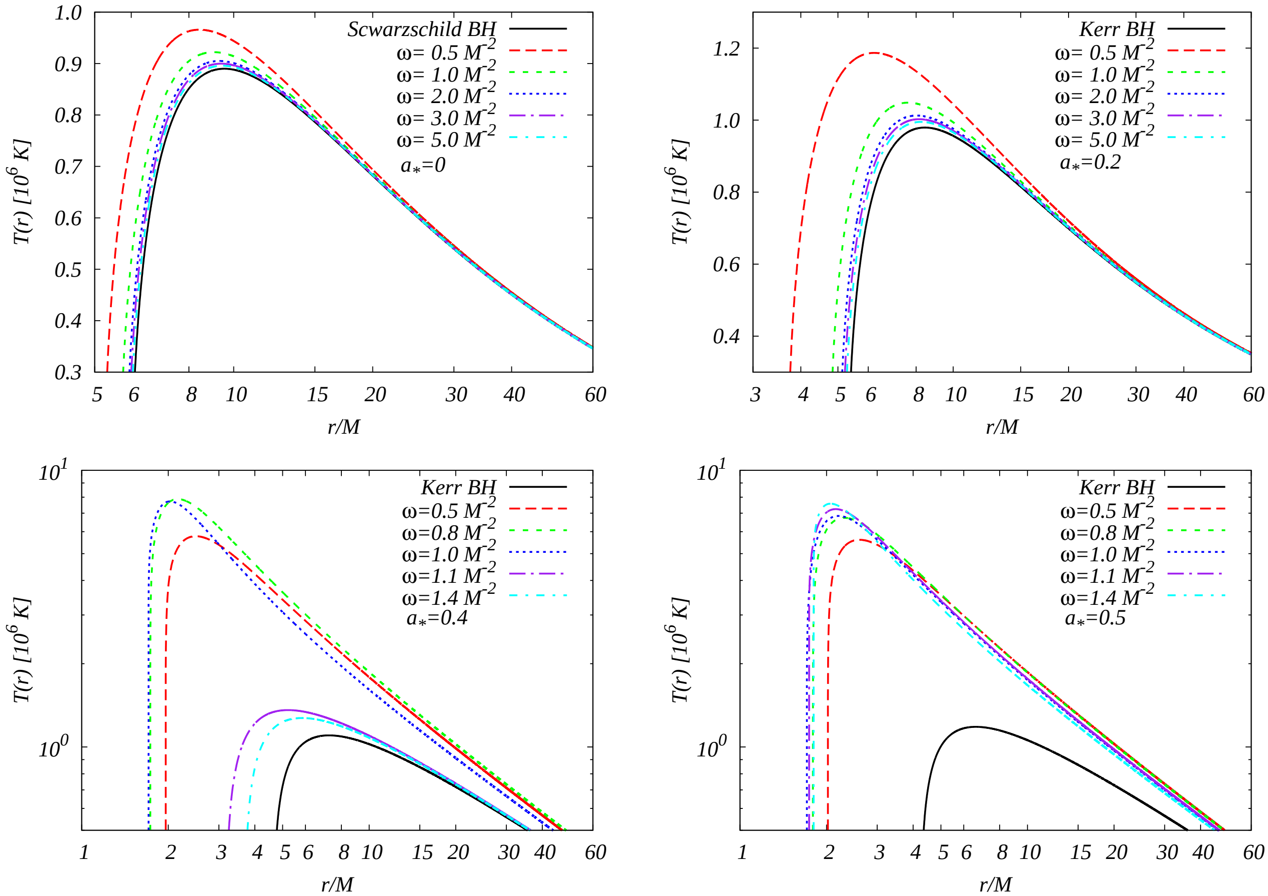

FIG. 4: The temperature profile of the disk around a static and a slowly rotating KS black hole with the total mass of $1M_\odot$ for different values of the parameters ω and a_*. The mass accretion rate is set to $10^{-12}M_\odot$/yr.

specific angular momentum and the rotational frequency have an explicit dependence on M in the form $\widetilde{L} \propto M$ and $\Omega \propto M^{-1}$, whereas $\tilde{E}$ does depend only on a_*. For any rescaling $M_2 = \alpha M_1$ of the mass of the KS black hole we obtain $x_2 = \alpha^{-1/2}x_1$ and the relations $\widetilde{E}(M_2)(x_2) = \widetilde{E}(M_1)(x_1)$, $\widetilde{L}(M_2)(x_2) = \alpha\widetilde{L}(M_1)(x_1)$ and $\Omega(M_2)(x_2) = \alpha^{-1}\Omega(M_1)(x_1)$. For the flux integral (A7) and for any rescaling $\dot{M}_0^{(2)} = \beta\dot{M}_0^{(1)}$ of the accretion rate these relations give

$$F(M_2, \dot{M}_0^{(2)})(x_2) = (\beta/\alpha^2)F(M_1, \dot{M}_0^{(1)})(x_1). \tag{29}$$

Then the temperature scales as

$$T(M_2, \dot{M}_0^{(2)})(x_2) = (\beta/\alpha^2)^{1/4}T(M_1, \dot{M}_0^{(1)})(x_1). \tag{30}$$

For the maximum of the luminosity L we have $\nu_{max} \propto T$ which gives $L(\nu_{max}) \propto \nu_{max}^3$. As the frequency scales with the temperature we obtain that

$$L(M_2, \dot{M}_0^{(2)})(\nu_2) = (\beta/\alpha^2)^{3/4}L(M_1, \dot{M}_0^{(1)})(\nu_1), \tag{31}$$

with

$$\nu_2(M_2, \dot{M}_0^{(2)}) = (\beta/\alpha^2)^{1/4}\nu_1(M_1, \dot{M}_0^{(1)}). \tag{32}$$

With the help of these scaling relations we can always obtain the values of the flux and of the luminosity for an arbitrary value of the mass, once these values are known for a given mass.

In Table I we present the conversion efficiency ϵ of the accreted mass into radiation for both the Kehagias-Sfestos and general relativistic black holes. As seen in Eq. (A8), the value of ϵ highly depends on the location of the inner edge of the disk. Under the critical value of the spin, r_{ms} shifts to lower radii for lower values of ω, and the efficiency obtained for the rotating Kehagias-Sfestos case is increasing as compared with the efficiency of the general relativistic black holes. By decreasing the value of ω, the efficiency increases, and the degree of this increase is enhanced for the black holes rotating at higher spin. If the latter is below the critical value of the spin, then this enhancement is inversely proportional to ω.

Above the critical value of the spin the inner edge of the disk is located at the event horizon, where $g_{tt} = 0$. In Fig. 2 we have also shown that Ω falls to zero at r_+. Then the specific energy given by Eq. (20) vanishes at the horizon. Since E_{ms} is zero at the inner edge of the disk, the particles deposited on the black hole carry

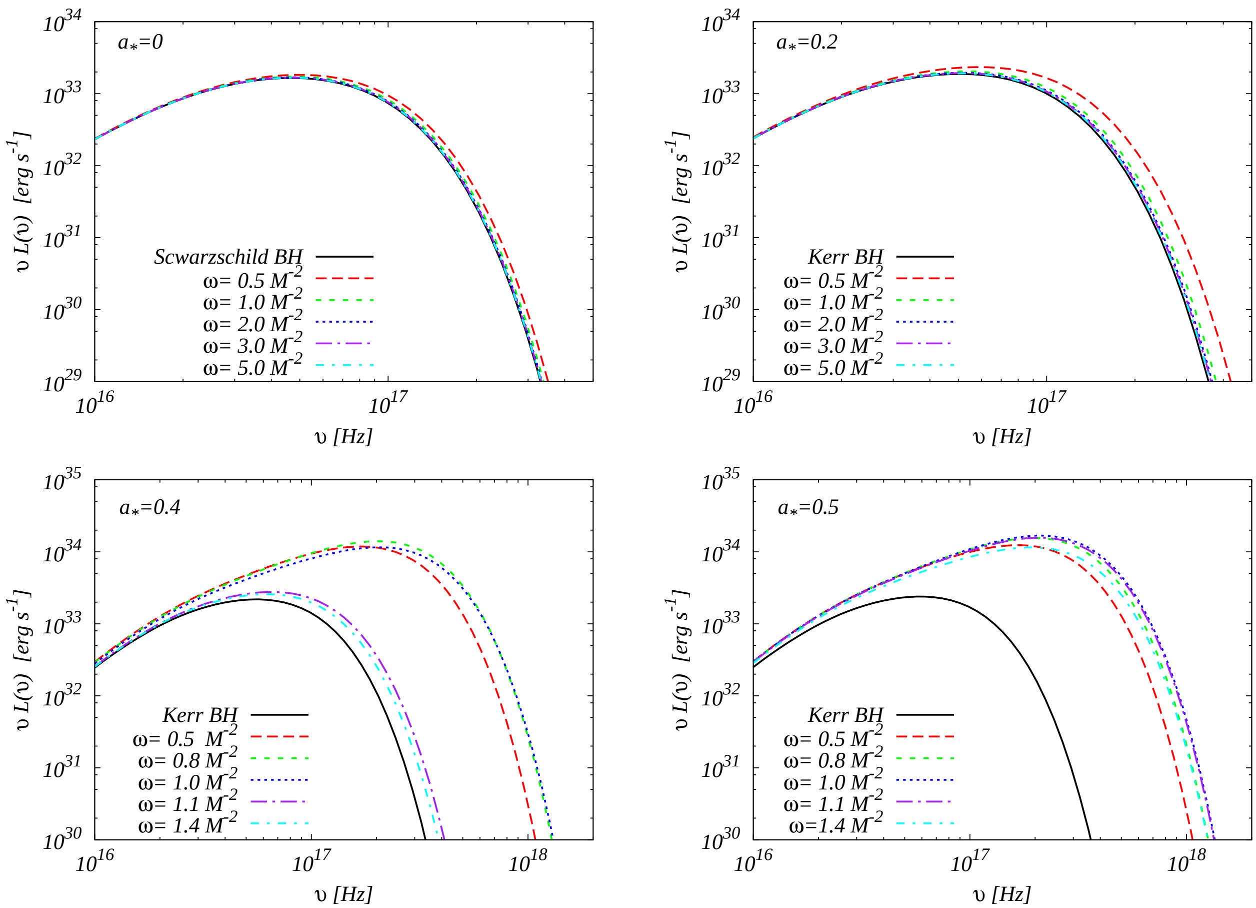

FIG. 5: The disk spectra for a static and a slowly rotating KS black hole with the total mass of $1M_{\odot}$ for different values of the parameters ω and a_*. The mass accretion rate is set to $10^{-12}M_{\odot}$/yr.

only their rest mass energy into the black hole, which is negligible as compared to the total thermal energy radiated by the disk. As a result, ϵ would essentially be one, i.e, the efficiency is 100% for spin values above the critical spin. However, we have also seen that the zone close to the inner edge of the disk cannot be cooled by thermal radiation only. Therefore in this case the application of the standard thin disk model is problematic. At its inner edge the disk may become geometrically thick, and other forms of the stress-energy, besides the specific energy and the specific angular momentum can play an important role in the mass-energy deposition. Then the usage of Eq. (A8) becomes problematic. We can still consider that, although the area of the forbidden radiative cooling, located between r_+ and r_{max} (the radius where Ω is maximal), is big enough to cause measurable effects in the energy-angular momentum transport between the black hole and the disk. However, this transport may still not determine drastic changes in the standard thin disk model. Hence, we expect that in this region the efficiency could still be very high, though not 100%.

Therefore, we conclude that the Kehagias-Sfetsos black holes convert accreted mass to radiation in a more efficient way than general relativistic black holes do. This enhancement in efficiency occurs even if the disk located around the rotating KS black holes can emit thermal photons only over some part of its entire surface area.

ω/M^2	$a_* = 0$	0.2	0.4	0.5
1/2	6.30 (5.28)	8.07 (3.72)	∼100 (1.71)	∼100 (1.00)
1	5.97 (5.66)	7.00 (4.78)	∼100 (1.71)	∼100 (1.00)
2	5.83 (5.84)	6.73 (5.06)	8.45 (3.97)	∼100 (1.00)
3	5.79 (5.89)	6.65 (5.14)	8.20 (4.15)	9.92 (3.35)
5	5.76 (5.94)	6.59 (5.21)	8.03 (4.26)	9.46 (3.59)
10	5.74 (6.00)	6.54 (5.29)	7.92 (4.37)	9.20 (3.73)
100	5.72 (6.00)	6.51 (5.29)	7.83 (4.45)	9.01 (3.84)
∞	5.72 (6.00)	6.46 (5.33)	7.51 (4.62)	8.21 (4.24)

TABLE I: The efficiency (measured in percents), and the values of the radius divided by M at the inner edge (values in parenthesis) of the accretion disk for slowly-rotating black holes in general relativity, and in the HL modified theory of gravity with the rotating KS solution. The case of $\omega \to \infty$ corresponds to the general relativistic case.

V. DISCUSSIONS AND FINAL REMARKS

In the present paper, we have studied thin accretion disk models for the slowly rotating Kehagias and Sfetsos black hole solution in Hořava gravity, and we have carried out an analysis of the properties of the radiation emerging from the surface of the disk. By comparing the accretion disk properties in the slowly rotating geometry in the Hořava-Lifshitz gravity with the properties of disks around a slowly rotating Kerr black hole, we have shown that the intensity of the flux emerging from the disk surface is greater for the slowly rotating Kehagias and Sfetsos solution than for the general relativistic rotating Kerr black hole with the same geometrical mass r_0 and accretion rate $\dot{M}_0$. If this difference is in the range of 20%-80% for the case of slowly rotating black holes, in the case of KS black holes with a_* of the order of $a_* = 0.4 - 0.5$, the increase in the flux could be several orders of magnitude higher than for a Kerr black hole. Thus extreme high energy emissions from accretion disks around black hole candidates may provide the distinctive signature for a KS black hole. We have also presented the conversion efficiency ϵ of the accreting mass into radiation, and we have showed that the slowly rotating Kehagias and Sfetsos black holes are much more efficient in converting the accreting mass into radiation than their Kerr black holes counterparts.

From an observational point of view, the determination of the mass and of the spin of the central compact general relativistic object is a very difficult task, and in many cases, their values are not known. Usually what is observed is the flux and the spectrum of the radiation coming from the accretion disk. Therefore, an essential problem that has to be considered is what properties of the radiation spectrum and flux, respectively, could indicate that the observed black hole is a Kehagias and Sfetsos black hole of the Hořava-Lifshitz gravity, rather than a standard Kerr black hole, with a different mass and spin. With the use of Eqs. (29)-(32) we can always describe the properties of the accretion disk in terms of an "effective" Kerr black hole, with a given "effective" mass and spin, respectively. Since for a Kehagias and Sfetsos black hole the emitted energy flux could be several orders of magnitude higher than for a Kerr black hole, for a given maximal value of a_*, the observed high flux from the Kehagias and Sfetsos black hole would require an unrealistically high mass for the central general relativistic compact object. Moreover, for the Kehagias and Sfetsos black hole the maximum of the flux is displaced toward smaller values of ν/M, as compared to the Kerr case. Hence a very high Kerr mass of the central object, and the position of the maximum of the spectrum could represent an important observational evidence for the existence of the Kehagias and Sfetsos black holes.

Therefore, the study of the accretion processes by compact objects is a powerful indicator of their physical nature. Since the energy flux, the temperature distribution of the disk, the spectrum of the emitted black body radiation, as well as the conversion efficiency show, in the case of the Hořava-Lifshitz theory vacuum solutions, significant differences as compared to the general relativistic case, the determination of these observational quantities could discriminate, at least in principle, between standard general relativity and Hořava-Lifshitz theory, and constrain the parameters of the model.

Acknowledgments

The work of TH is supported by an RGC grant of the government of the Hong Kong SAR. FSNL acknowledges financial support of the Fundação para a Ciência e Tecnologia through the grants PTDC/FIS/102742/2008 and CERN/FP/109381/2009.

Appendix A: Physical properties of thin accretion disks

For a thin accretion disk the vertical size (defined in cylindrical coordinates along the z-axis) is negligible, as compared to its horizontal extension (defined along the radial direction r), i.e., the disk height H, equal to the maximum half thickness of the disk, is always much smaller than the characteristic radius R of the disk, $H \ll R$. The thin disk is assumed to be in hydrodynamical equilibrium, and the pressure gradient, as well as the vertical entropy gradient, are negligible in the disk. The efficient cooling via the radiation over the disk surface prevents the disk from cumulating the heat generated by stresses and dynamical friction. In turn, this equilibrium causes the disk to stabilize its thin vertical size. The thin disk has an inner edge at the marginally stable orbit of the compact object potential, and the accreting matter has a Keplerian motion in higher orbits.

In steady-state accretion disk models, the mass accretion rate $\dot{M}_0$ is assumed to be a constant that does not change with time. The physical quantities describing the orbiting matter are averaged over a characteristic time scale, e.g. Δt, for a total period of the orbits, over the azimuthal angle $\Delta\phi = 2\pi$, and over the height H [21–23].

The particles moving in Keplerian orbits around the compact object with a rotational velocity $\Omega = d\phi/dt$ have a specific energy $\widetilde{E}$ and a specific angular momentum $\widetilde{L}$, which in the steady-state thin disk model depend only on the radii of the orbits. These particles, orbiting with the four-velocity u^μ, form a disk of an averaged surface density Σ, the vertically integrated average of the rest mass density ρ_0 of the plasma. The accreting matter in the disk is modeled by an anisotropic fluid source, where the density ρ_0, the energy flow vector q^μ and the stress tensor $t^{\mu\nu}$ are measured in the averaged rest-frame (the specific heat was neglected). Then, the disk structure can be characterized by the surface density of the disk

[21, 23]

$$\Sigma(r) = \int_{-H}^{H} \langle \rho_0 \rangle dz, \tag{A1}$$

with averaged rest mass density $\langle \rho_0 \rangle$ over Δt and 2π and the torque

$$W_{\phi}{}^{r} = \int_{-H}^{H} \langle t_{\phi}{}^{r} \rangle dz, \tag{A2}$$

with the averaged component $\langle t^r_\phi \rangle$ over Δt and 2π. The time and orbital average of the energy flux vector gives the radiation flux $F(r)$ over the disk surface as $F(r) = \langle q^z \rangle$.

The stress-energy tensor is decomposed according to

$$T^{\mu\nu} = \rho_0 u^\mu u^\nu + 2u^{(\mu} q^{\nu)} + t^{\mu\nu}, \tag{A3}$$

where $u_\mu q^\mu = 0$, $u_\mu t^{\mu\nu} = 0$. The four-vectors of the energy and angular momentum flux are defined by $-E^\mu \equiv T^\mu_\nu (\partial/\partial t)^\nu$ and $J^\mu \equiv T^\mu_\nu (\partial/\partial\phi)^\nu$, respectively. The structure equations of the thin disk can be derived by integrating the conservation laws of the rest mass, of the energy, and of the angular momentum of the plasma, respectively [21, 23]. From the equation of the rest mass conservation, $\nabla_\mu(\rho_0 u^\mu) = 0$, it follows that the time averaged rate of the accretion of the rest mass is independent of the disk radius,

$$\dot{M}_0 \equiv -2\pi r \Sigma u^r = \text{constant}. \tag{A4}$$

Applying the conservation law $\nabla_\mu E^\mu = 0$ of the energy has the integral form

$$[\dot{M}_0 \widetilde{E} - 2\pi r \Omega W_{\phi}{}^{r}]_{,r} = 4\pi r F \widetilde{E}, \tag{A5}$$

which states that the energy transported by the rest mass flow, $\dot{M}_0 \widetilde{E}$, and the energy transported by the dynamical stresses in the disk, $2\pi r \Omega W_{\phi}{}^{r}$, is in balance with the energy radiated away from the surface of the disk, $4\pi r F \widetilde{E}$. The law of the angular momentum conservation, $\nabla_\mu J^\mu = 0$, also states the balance of these three forms of the angular momentum transport,

$$[\dot{M}_0 \widetilde{L} - 2\pi r W_{\phi}{}^{r}]_{,r} = 4\pi r F \widetilde{L}. \tag{A6}$$

By eliminating $W_{\phi}{}^{r}$ from Eqs. (A5) and (A6), and applying the universal energy-angular momentum relation $dE = \Omega dJ$ for circular geodesic orbits in the form $\widetilde{E}_{,r} = \Omega \widetilde{L}_{,r}$, the flux F of the radiant energy over the disk can be expressed in terms of the specific energy, angular momentum and of the angular velocity of the compact sphere [21, 23],

$$F(r) = -\frac{\dot{M}_0}{4\pi\sqrt{-g}} \frac{\Omega_{,r}}{(\widetilde{E} - \Omega \widetilde{L})^2} \int_{r_{ms}}^{r} (\widetilde{E} - \Omega \widetilde{L}) \widetilde{L}_{,r} dr. \tag{A7}$$

Another important characteristic of the mass accretion process is the efficiency with which the central object converts rest mass into outgoing radiation. This quantity is defined as the ratio of the rate of the radiation of the energy of photons escaping from the disk surface to infinity, and the rate at which mass-energy is transported to the central compact general relativistic object, both measured at infinity [21, 23]. Since the former is given by the rate of the difference between the total mass growth of the central object and the accreted rest mass, the efficiency can be written as $\epsilon = (\Delta M - \Delta M_0)/\Delta M_0$. The accretion of the rest mass ΔM_0 producing a growth in the total mass-energy of the central object proportional to the specific energy of the gas particles leaving the marginally stable orbit, i.e $\Delta M = \widetilde{E}_{ms} \Delta M_0$. Therefore the efficiency is given in terms of the specific energy measured at the marginally stable orbit r_{ms},

$$\epsilon = 1 - \widetilde{E}_{ms}, \tag{A8}$$

provided all the emitted photons can escape to infinity.

For Schwarzschild black holes the efficiency ϵ is about 6%, whether the photon capture by the black hole is considered, or not. Ignoring the capture of radiation by the hole, ϵ is found to be 42% for rapidly rotating black holes, whereas the efficiency is 40% with photon capture in the Kerr potential [24].

The accreting matter in the steady-state thin disk model is supposed to be in thermodynamical equilibrium. Therefore the radiation emitted by the disk surface can be considered as a perfect black body radiation, where the energy flux is given by $F(r) = \sigma T^4(r)$ (σ is the Stefan-Boltzmann constant), and the observed luminosity $L(\nu)$ has a redshifted black body spectrum [29]:

$$L(\nu) = 4\pi d^2 I(\nu) = \frac{8}{\pi} \cos\gamma \int_{r_i}^{r_f} \int_0^{2\pi} \frac{\nu_e^3 r d\phi dr}{\exp(h\nu_e/T) - 1}. \tag{A9}$$

Here d is the distance to the source, $I(\nu)$ is the Planck distribution function, γ is the disk inclination angle, and r_i and r_f indicate the position of the inner and outer edge of the disk, respectively. We take $r_i = r_{ms}$ and $r_f \to \infty$, since we expect the flux over the disk surface vanishes at $r \to \infty$ for any kind of general relativistic compact object geometry. The emitted frequency is given by $\nu_e = \nu(1+z)$, and the redshift factor can be written as

$$1 + z = \frac{1 + \Omega r \sin\phi \sin\gamma}{\sqrt{-g_{tt} - 2\Omega g_{t\phi} - \Omega^2 g_{\phi\phi}}}, \tag{A10}$$

where we have neglected the light bending [36, 37].

[1] P. Horava, JHEP **0903**, 020 (2009).
[2] P. Horava, Phys. Rev. D **79**, 084008 (2009).
[3] T. P. Sotiriou, M. Visser and S. Weinfurtner, Phys. Rev. Lett. **102**, 251601 (2009); M. Visser, Phys. Rev. **D80**, 025011 (2009); P. Horava, Phys. Rev. Lett. **102**, 161301 (2009); R. G. Cai, Y. Liu and Y. W. Sun, JHEP **0906**, 010 (2009); B. Chen and Q. G. Huang, arXiv:0904.4565 [hep-th]; D. Orlando and S. Reffert, Class. Quant. Grav. **26**, 155021 (2009); R. G. Cai, B. Hu and H. B. Zhang, Phys. Rev. **D80**, 041501 (2009); T. Nishioka, Class. Quant. Grav. **26**, 242001 (2009); M. Li and Y. Pang, JHEP **0908**, 015 (2009); C. Charmousis, G. Niz, A. Padilla and P. M. Saffin, JHEP **0908**, 070 (2009); T. P. Sotiriou, M. Visser and S. Weinfurtner, JHEP **0910**, 033 (2009); G. Calcagni, Phys. Rev. **D81**, 044006, (2010); D. Blas, O. Pujolas and S. Sibiryakov, JHEP **0910**, 029 (2009); R. Iengo, J. G. Russo and M. Serone, JHEP **0911**, 020 (2009); C. Germani, A. Kehagias and K. Sfetsos, JHEP **09**, 060 (2009); S. Mukohyama, JCAP **0909**, 005 (2009); A. Kobakhidze, Phys. Rev. **D82**, 064011 (2010); C. Appignani, R. Casadio and S. Shankaranarayanan, JCAP **04**, 006 (2010); J. Kluson, JHEP **0911**, 078 (2009); N. Afshordi, Phys. Rev. **D80**, 081502 (2009); A. Kocharyan, Phys. Rev. **D 80**, 024026 (2009); D. Orlando and S. Reffert, Phys. Lett. B **683**, 62 (2010); D. Blas, O. Pujolas and S. Sibiryakov, Phys. Rev. Lett. **104**, 181302 (2010); M. i. Park, Class. Quant. Grav. **28**, 015004 (2011); K. Koyama and F. Arroja, JHEP **1003**, 061 (2010); M. i. Park, arXiv:0910.5117 [hep-th]; A. Papazoglou and T. P. Sotiriou, Phys. Lett. **B685**, 197 (2010); M. Henneaux, A. Kleinschmidt and G. L. Gomez, Phys.Rev. **D81**, 064002 (2010); M. Visser, arXiv:0912.4757 [hep-th].
[4] T. Takahashi and J. Soda, Phys. Rev. Lett. **102**, 231301 (2009); G. Calcagni, JHEP **09**, 112 (2009); E. Kiritsis and G. Kofinas, Nucl. Phys. **B821**, 467 (2009); S. Mukohyama, JCAP **0906**, 001 (2009); R. Brandenberger, arXiv:0904.2835 [hep-th]; Y. S. Piao, Phys. Lett. **B681**, 1 (2009); X. Gao, arXiv:0904.4187 [hep-th]; S. Mukohyama, K. Nakayama, F. Takahashi and S. Yokoyama, Phys. Lett. **B679**, 6 (2009); S. Kalyana Rama, Phys. Rev. **D79**, 124031 (2009); B. Chen, S. Pi and J. Z. Tang, JCAP **0908**, 007 (2009); X. Gao, Y. Wang, R. Brandenberger and A. Riotto, Phys. Rev. **D81**, 083508 (2010); M. Minamitsuji, Phys. Lett. **B684**, 194 (2010); A. Wang and Y. Wu, JCAP **0907**, 012 (2009); S. Nojiri and S. D. Odintsov, Phys. Rev. **D81**, 043001 (2010); Y. F. Cai and E. N. Saridakis, JCAP **0910**, 020 (2009); A. Wang and R. Maartens, Phys. Rev. **D81**, 024009 (2010); T. Kobayashi, Y. Urakawa and M. Yamaguchi, JCAP **0911**, 015 (2009); P. Wu and H. W. Yu, Phys. Rev. **D81**, 103522 (2010); C. G. Boehmer and F. S. N. Lobo, Eur. Phys. J. **C70**, 1111 (2010); T. Kobayashi, Y. Urakawa and M. Yamaguchi, JCAP **0911**, 015 (2009) [arXiv:0908.1005 [astro-ph.CO]]; S. Maeda, S. Mukohyama and T. Shiromizu, Phys. Rev. D **80**, 123538 (2009); S. Carloni, E. Elizalde and P. J. Silva, arXiv:0909.2219 [hep-th]; G. Leon and E. N. Saridakis, JCAP **0911**, 006 (2009); A. Wang, D. Wands and R. Maartens, JCAP **1003**, 013 (2010); B. Chen, S. Pi and J. Z. Tang, arXiv:0910.0338 [hep-th]; D. Momeni, arXiv:0910.0594 [gr-qc]; R. G. Cai and N. Ohta, arXiv:0910.2307 [hep-th]; R. A. Porto and A. Zee, arXiv:0910.3716 [hep-th]; S. Dutta and E. N. Saridakis, JCAP **1001**, 013 (2010) [arXiv:0911.1435 [hep-th]]; I. Bakas, F. Bourliot, D. Lust and M. Petropoulos, arXiv:0911.2665 [hep-th]; X. Gao, Y. Wang, W. Xue and R. Brandenberger, arXiv:0911.3196 [hep-th]; E. Czuchry, arXiv:0911.3891 [hep-th]; R. Garattini, arXiv:0912.0136 [gr-qc]; M. Wang, J. Jing, C. Ding and S. Chen, arXiv:0912.4832 [gr-qc]; R. G. Cai and A. Wang, arXiv:1001.0155 [hep-th]; M. R. Setare and M. Jamil, arXiv:1001.1251 [hep-th]; C. G. Boehmer, L. Hollenstein, F. S. N. Lobo and S. S. Seahra, arXiv:1001.1266 [gr-qc]; Q. J. Cao, Y. X. Chen and K. N. Shao, arXiv:1001.2597 [hep-th].
[5] E. N. Saridakis, arXiv:0905.3532 [hep-th]; M. i. Park, arXiv:0906.4275 [hep-th]. M. R. Setare, arXiv:0909.0456 [hep-th];
[6] S. Mukohyama, arXiv:0905.3563 [hep-th].
[7] H. Nastase, arXiv:0904.3604 [hep-th]; R. G. Cai, L. M. Cao and N. Ohta, Phys. Rev. **D80**, 024003 (2009); Y. S. Myung and Y. W. Kim, arXiv:0905.0179 [hep-th]; R. G. Cai, L. M. Cao and N. Ohta, arXiv:0905.0751 [hep-th]; R. B. Mann, JHEP **0906**, 075 (2009); R. A. Konoplya, Phys. Lett. **B679**, 499 (2009); S. Chen and J. Jing, Phys. Rev. **D80**, 024036 (2009); J. Chen and Y. Wang, arXiv:0905.2786 [gr-qc]; S. Chen and J. Jing, arXiv:0905.1409 [gr-qc]; M. Botta-Cantcheff, N. Grandi and M. Sturla, arXiv:0906.0582 [hep-th]; A. Castillo and A. Larranaga, arXiv:0906.4380 [gr-qc]; J. J. Peng and S. Q. Wu, arXiv:0906.5121 [hep-th]. E. O. Colgain and H. Yavartanoo, JHEP **0908**, 021 (2009); H. W. Lee, Y. W. Kim and Y. S. Myung, arXiv:0907.3568 [hep-th]; S. S. Kim, T. Kim and Y. Kim, arXiv:0907.3093 [hep-th]; Y. S. Myung, arXiv:0908.4132 [hep-th]; C. Ding, S. Chen and J. Jing, arXiv:0909.2490 [gr-qc]; J. Z. Tang and B. Chen, arXiv:0909.4127 [hep-th]; N. Varghese and V. C. Kuriakose, arXiv:0909.4944 [gr-qc]; D. Y. Chen, H. Yang and X. T. Zu, Phys. Lett. B **681**, 463 (2009); E. Kiritsis and G. Kofinas, arXiv:0910.5487 [hep-th]; T. Harada, U. Miyamoto and N. Tsukamoto, arXiv:0911.1187 [gr-qc]; M. R. Setare and D. Momeni, arXiv:0911.1877 [hep-th];
[8] K. Izumi and S. Mukohyama, arXiv:0911.1814 [hep-th];
[9] D. Capasso and A. P. Polychronakos, arXiv:0911.1535 [hep-th]; E. Kiritsis, arXiv:0911.3164 [hep-th]; B. R. Majhi, arXiv:0911.3239 [hep-th]; J. Z. Tang, arXiv:0911.3849 [hep-th]; R. G. Cai and H. Q. Zhang, arXiv:0911.4867 [hep-th]; J. Greenwald, A. Papazoglou and A. Wang, arXiv:0912.0011 [hep-th]; Y. S. Myung, arXiv:0912.3305 [hep-th];
[10] M. i. Park, arXiv:0905.4480 [hep-th].
[11] H. Lu, J. Mei and C. N. Pope, Phys. Rev. Lett. **103**, 091301 (2009).
[12] A. Kehagias and K. Sfetsos, Phys. Lett. **B678**, 123 (2009).
[13] A. Ghodsi and E. Hatefi, arXiv:0906.1237 [hep-th].
[14] R. A. Konoplya, arXiv:0905.1523 [hep-th].
[15] S. Chen and J. Jing, arXiv:0905.2055 [gr-qc].
[16] J. Chen and Y. Wang, arXiv:0905.2786 [gr-qc].
[17] T. Harko, Z. Kovacs and F. S. N. Lobo, Phys. Rev. D

80, 044021 (2009).

[18] H. W. Lee, Y. W. Kim and Y. S. Myung, Eur. Phys. J. C **70**, 367 (2010).

[19] C. M. Urry and P. Padovani, Publ. Astron. Soc. of the Pacific **107**, 803 (1995).

[20] M. Miyoshi, J. Moran, J. Herrnstein, L. Greenhill, N. Nakai, P. Diamond and M. Inoue, Nature **373**, 127 (1995).

[21] I. D. Novikov and K. S. Thorne, in Black Holes, ed. C. DeWitt and B. DeWitt, New York: Gordon and Breach (1973).

[22] N. I. Shakura and R. A. Sunyaev, Astron. Astrophys. **24**, 33 (1973).

[23] D. N. Page and K. S. Thorne, Astrophys. J. **191**, 499 (1974).

[24] K. S. Thorne, Astrophys. J. **191**, 507 (1974).

[25] T. Harko, Z. Kovacs and F. S. N. Lobo, Phys. Rev. **D78**, 084005 (2008).

[26] T. Harko, Z. Kovacs and F. S. N. Lobo, Phys. Rev. D **79**, 064001 (2009).

[27] S. Bhattacharyya, A. V. Thampan and I. Bombaci, Astron. Astrophys. **372**, 925 (2001).

[28] Z. Kovacs, K. S. Cheng and T. Harko, Astron. Astrophys. **500**, 621 (2009).

[29] D. Torres, Nucl. Phys. B **626**, 377 (2002).

[30] Y. F. Yuan, R. Narayan and M. J. Rees Astrophys. J. **606**, 1112 (2004).

[31] F. S. Guzman, Phys. Rev. D **73**, 021501 (2006).

[32] C. S. J. Pun, Z. Kovacs and T. Harko, Phys. Rev. **D78**, 084015 (2008).

[33] T. Harko, Z. Kovacs and F. S. N. Lobo, Class. Quant. Grav. **26**, 215006 (2009).

[34] T. Harko, Z. Kovacs and F. S. N. Lobo, Class. Quant. Grav. **27**, 105010 (2010).

[35] C. S. J. Pun, Z. Kovacs and T. Harko, Phys. Rev. D **78**, 024043 (2008).

[36] J. P. Luminet, Astron. Astrophys. **75**, 228 (1979).

[37] S. Bhattacharyya, R. Misra and A. V. Thampan, Astrophys. J. **550**, 841 (2001).

[38] K. S. Thorne and R. H. Price, Astrophys. J. **195**, L101 (1975).

[39] E. T. P. Liang and R. H. Price, Astrophys. J. **218**, 247 (1977).